# Fiber-Optic Sensors Based on Surface Plasmon Resonance: A Comprehensive Review

Anuj K. Sharma, Rajan Jha, and B. D. Gupta

***Abstract*—Since the introduction of optical fiber technology in the field of sensor based on the technique of surface plasmon resonance (SPR), fiber-optic SPR sensors have witnessed a lot of advancements. This paper reports on the past, present, and future scope of fiber-optic SPR sensors in the field of sensing of different chemical, physical, and biochemical parameters. A detailed mechanism of the SPR technique for sensing purposes has been discussed. Different new techniques and models in this area that have been introduced are discussed in quite a detail. We have tried to put the different advancements in the order of their chronological evolution. The content of the review article may be of great importance for the research community who are to take the field of fiber-optic SPR sensors as its research endeavors.**

***Index Terms*—Optical fiber, sensitivity, sensor, signal-to-noise ratio (SNR), surface plasmon resonance (SPR).**

## I. Introduction

THE ORIGIN OF the phenomenon of surface plasmon resonance (SPR) is almost a century old. In 1907, Zenneck formulated a special surface wave solution to Maxwell's equations and demonstrated, theoretically, that radio frequency surface EM waves occur at the boundary of two media when one medium is either a "lossy" dielectric, or a metal, and the other is a loss-free medium [1]. Zenneck also suggested that it is the "lossy" (imaginary) part of the dielectric function that is responsible for binding the EM wave to the interface. In 1909, Sommerfeld found that the field amplitudes of surface waves postulated by Zenneck varied inversely as the square root of the horizontal distance from the source dipole [2]. Furthermore, it was a fast wave and it decayed exponentially with height above the interface. However, the real progress to the phenomenon of SPR was made in 1957 when Ritchie theoretically demonstrated the existence of surface plasma excitations at a metal surface [3]. In 1960, Powell and Swan observed the excitation of surface plasmons at metal interfaces using electrons [4]. Soon after, Stern and Ferrell showed that surface electromagnetic waves at a metallic surface involved electromagnetic radiation coupled to surface plasmons [5]. They also derived the dispersion relations for electromagnetic surface waves at metal surfaces. Further, in 1968, Otto devised the attenuated total reflection (ATR) prism coupling method to enable the coupling of bulk electromagnetic light wave with surface electromagnetic waves [6]. The Otto configuration, due to a finite gap between prism base and metal layer, was more suited to the surfaces, which would not be damaged or touched by the prism and is important for the study of single-crystal surfaces. Kretschmann [7] modified the Otto configuration and is the most famous configuration for the excitation of surface plasmons till date. In the Kretschmann configuration, a thin metal layer with a thickness of the order of 10–100 nm contacts the prism base.

While presenting this review, we already have a few important reviews in the related areas. For instance, one of them focusing only on SPR sensors, outlined main application areas and presented important examples of applications of SPR sensor technology [8]. Another review concerns the analysis of the performance of other techniques (interferometry and luminescence) along with SPR in chemical and biological sensors [9]. Performance parameters were compared for the sensing techniques of interferometry, SPR, and luminescence. A detailed explanation of the physical and chemical/biological properties required for optical sensors was included along with the principle of operation of the sensors. Another review highlighted the status of different fiber-optic chemical sensors and biosensors [10]. However, a separate review for optical fiber-based SPR sensors is absent. In the present paper, we review SPR-based fiber-optic sensors with two main objectives. First, we are inclined to provide a systematic and comprehensive introduction to the technique of SPR for researchers (particularly, new students) who plan to carry out research in the field of SPR-based sensors. Second, we wish to highlight the role of optical fibers in efficient and flexible SPR sensors because fiber-optic-based SPR sensors have excessively more advantages over the conventional prism-based SPR sensors. In the end we provide a detailed discussion on emerging techniques and fields in the area of fiber-optic SPR sensors.

The organization of review is as follows. A brief but necessary history of SPR is given in Section I. The phenomenon of SPR is described in great detail along with the explanations of very fine technical points. The description of SPR is followed by its application for sensing purposes. The main performance parameters of SPR sensors are discussed along with their definitive points. The feasibility of optical fibers in SPR sensors is discussed, which is then followed by the general configuration of fiber-optic SPR sensors. Finally, past and present of the fiber-optic SPR sensors is discussed in sufficient detail until the end of the year 2006. In the end, we provide the future scope of research and development of fiber-optic SPR sensors.

## II. Surface Plasmon Resonance

### A. Plasmons or Plasma Oscillations

There is a dense assembly of negatively charged free electrons inside a conductor (free electron charge density is $10^{23}$ cm$^{-3}$ and, therefore, the group of free electrons can be compared with

Manuscript received March 1, 2007; accepted March 4, 2007. This work was supported in part by the CSIR under Grant 03(1025)/05/EMR-II. The associate editor coordinating the review of this paper and approving it for publication was Prof. Krishna Persaud.

The authors are with the Indian Institute of Technology, New Delhi 110016, India (e-mail: anujsharma@gmail.com).

Digital Object Identifier 10.1109/JSEN.2007.897946

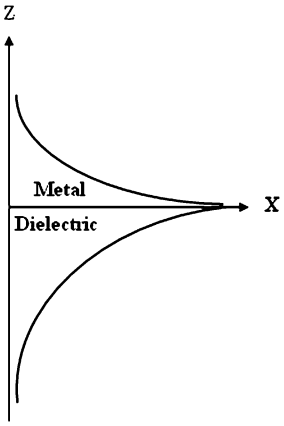


Fig. 1. Exponential decay of field intensity of surface plasmon mode in a metal and dielectric system.

a plasma of particles), and also an equally charged positive ion lattice. Since, positive ions have an infinitely large mass compared with these free electrons, therefore, according to the jellium model, these ions can be replaced by a positive constant background. However, the total charge density inside the conductor still remains to be zero. If the density of free electrons is locally reduced by applying an external field on the conductor so that the movement of free electrons may take place, the negative free electrons are no longer screened by the background and they begin to get attracted by the positive ion background. This attraction acts as a driving force for free electrons and they move to positive region and accumulate with a density greater than necessary to obtain charge neutrality. Now, at this point, the Coulomb repulsion among the moving free electrons acts as a restoring force and produces motion in opposite direction. The resultant of the two forces (i.e., attractive driving force and repulsive restoring force) set up the longitudinal oscillations among the free electrons. These oscillations are known as plasma oscillations. A plasmon is a quantum of the plasma oscillation. The existence of plasma oscillations has been demonstrated in electron energy-loss experiments [3], [4].

### *B. Surface Plasmons*

A metal-dielectric interface supports plasma oscillations. These charge density oscillations along the metal-dielectric interface are known as surface plasma oscillations. The quantum of these oscillations is referred to as surface plasmon (also a surface plasmon wave or a surface plasmon mode). These surface plasmons are accompanied by a longitudinal (TM- or p-polarized) electric field, which decays exponentially in metal as well as dielectric (Fig. 1). Due to this exponential decay of field intensity, the field has its maximum at metal-dielectric interface itself. Both of these crucial properties of surface plasmons being TM-polarized and exponential decay of electric field are found by solving the Maxwell's equation for metal-dielectric kind of refractive index distribution. By the solution of Maxwell's equation, one can also show that the surface plasmon wave propagation constant $(K_{\mathrm{SP}})$ is continuous through the metal-dielectric interface and is given by

$$K_{\mathrm{SP}} = \frac{\omega}{c}\left(\frac{\varepsilon_m \varepsilon_s}{\varepsilon_m + \varepsilon_s}\right)^{1/2} \tag{1}$$

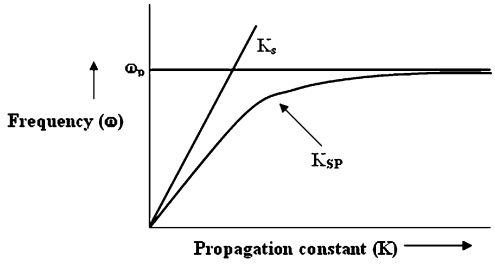


Fig. 2. Dispersion curves for surface plasmon wave $(K_{\mathrm{SP}})$ and the direct light incident through the dielectric medium $(K_s)$. $\omega_p$ is the plasma frequency of metal layer.

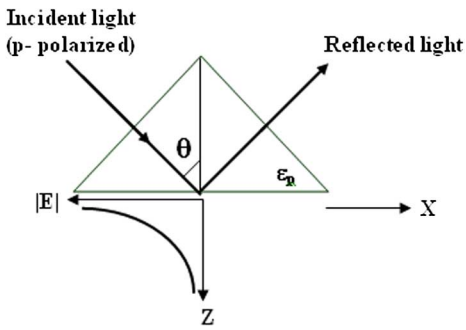


Fig. 3. Illustration of setting up of an evanescent wave at prism-metal interface at $\theta > \theta_{\mathrm{ATR}}$.

where $\varepsilon_m$ and $\varepsilon_s$ represent the dielectric constants of metal layer and the dielectric medium; $\omega$ represents the frequency of incident light, and $c$ is the velocity of light. The above equation implies that the properties of surface plasmon wave vector depend on both media, i.e., metal and dielectric.

### *C. Excitation of Surface Plasmons by Light*

The maximum propagation constant of the light wave at frequency $\omega$ propagating through the dielectric medium is given by

$$K_s = \frac{\omega}{c}\sqrt{\varepsilon_s}. \tag{2}$$

Since $\varepsilon_m < 0$ (i.e., for metal) and $\varepsilon_s > 0$ (i.e., for dielectric), for a given frequency, the propagation constant of surface plasmon is greater than that of the light wave (of same polarization state as that of the surface plasmon wave, i.e., p-polarized) in dielectric medium (Fig. 2). Hence, the direct light cannot excite surface plasmons at a metal-dielectric interface and is referred to as nonradiative surface plasmon. Therefore, to excite surface plasmons, the momentum and hence the wave vector of the exciting light in dielectric medium should be increased. In other words, an extra momentum (and energy) must be imparted to light wave in order to get the surface plasmons excited at a metal-dielectric interface.

### *D. Otto Configuration*

The general idea behind this configuration was the coupling of surface plasmon wave with the evanescent wave, which is set up due to ATR at the base of a coupling prism when a light beam is incident at an angle greater than the critical angle $(\theta_{\mathrm{ATR}})$ at prism-air interface [6] (Fig. 3). The nature of evanescent wave is known to have the propagation constant along the interface and to decay exponentially in the dielectric medium adjacent to metal layer. Both of these characteristics of evanescent wave

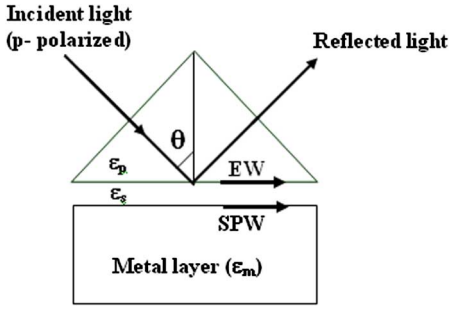


Fig. 4. Otto configuration for the excitation of surface plasmons at metal-dielectric interface.

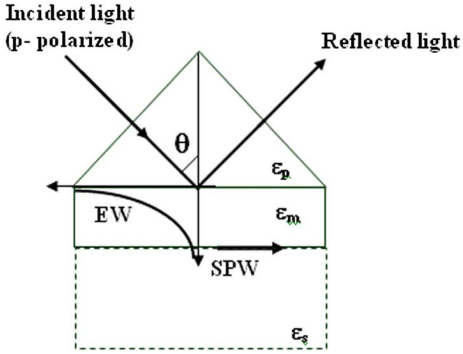


Fig. 5. Kretschmann configuration for the excitation of surface plasmons at metal-dielectric interface.

are similar to those of a surface plasmon wave, therefore, there is a strong possibility of interaction between these waves. The x-component of the wave propagation constant of the evanescent wave at prism-air interface is given by

$$K_{\mathrm{ev}} = \frac{\omega}{c}\sqrt{\varepsilon_p}\sin\theta. \tag{3}$$

If a metal surface is now brought in contact of this decaying evanescent field in such a way that an air gap remains between the prism base and metal layer, then the evanescent field at prism-air interface can excite the surface plasmons at the air-metal interface (Fig. 4). However, this configuration is difficult to realize practically as the metal has to be brought within around 200 nm of the prism surface. This approach has been found to be very useful in studying the single-crystal metal surfaces and adsorption on them.

### *E. Kretschmann–Reather ATR Method*

As a significant improvement to Otto configuration, Kretschmann and Reather realized that the metal layer could be used as the spacing layer, i.e., evanescent wave (an exponentially decaying wave propagating along the interface of two media due to the occurrence of total internal reflection) generated at the prism-metal layer interface can excite surface plasmons at the metal-air interface so long as the metal layer thickness is not too large. They devised a new configuration [7], given in Fig. 5. In this configuration as well, surface plasmons are excited by an evanescent wave from a high refractive index glass prism at ATR condition. However, unlike Otto configuration, the base of the glass prism is coated with a thin metal film (typically around 50 nm thick) and is kept in direct contact with

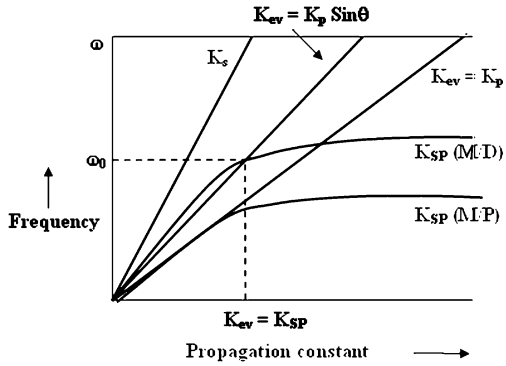


Fig. 6. Dispersion curves for direct light wave in dielectric $(K_s)$, evanescent wave $(K_{\mathrm{ev}})$ for $\theta = \theta_{\mathrm{ATR}}$ and $\theta = 90°$, surface plasmon wave $K_{\mathrm{SP}}$ at metal-dielectric interface (M/D) and at metal-prism interface (M/P).

the dielectric medium of lower refractive index (such as air or some other dielectric sample). When a p-polarized light beam is incident through the prism on the prism-metal layer interface at an angle $\theta$ equal to or greater than the angle required for ATR $(\theta_{\mathrm{ATR}})$, the evanescent wave is generated at the prism-metal layer interface. Fig. 6 shows the dispersion curves of the surface plasmon along with those of the direct light and the light incident through a glass prism of higher refractive index. The wave vector $K_{\mathrm{ev}}$ of the evanescent wave, corresponding to incident angle $\theta$, is equal to the lateral component of the wave vector of the incident light in the prism, as given in (3). The excitation of surface plasmon occurs when the wave vector of the propagation constant of evanescent wave exactly matches with that of the surface plasmon of similar frequency and state of polarization. This occurs at a particular angle of incidence $\theta_{\mathrm{res}}$ and the corresponding resonance condition for surface plasmons is written as

$$\frac{\omega}{c}\sqrt{\varepsilon_p}\mathrm{Sin}\theta_{\mathrm{res}} = \frac{\omega}{c}\left(\frac{\varepsilon_m\varepsilon_s}{\varepsilon_m+\varepsilon_s}\right)^{1/2}. \tag{4}$$

Fig. 6 clearly shows that the propagation constant curves corresponding to surface plasmon wave and evanescent wave cross each other at many positions lying between $K_{\mathrm{ev}} = K_p\mathrm{Sin}\theta$ and $K_{\mathrm{ev}} = K_p$ [i.e., for different sets of angle of incidence and frequency $(\theta,\omega)$]. This implies that the propagation constant of evanescent wave $(K_{\mathrm{ev}})$ may match with that of the surface plasmon wave (at the metal-dielectric interface M/D) depending on the frequency and angle of incidence of light beam. As a very important observation, the surface plasmon wave propagation constant for metal-prism interface (M/P) lies to right of the maximum propagation constant of evanescent wave $(K_{\mathrm{ev}} = K_p)$, and the two curves never cross each other. This suggests that there is no excitation of surface plasmons at metal-prism interface.

### *F. Minimum of Reflectance at Resonance*

The excitation of surface plasmons at metal-dielectric interface results in the transfer of energy from incident photons to surface plasmons, which reduces the energy of the reflected light. If the normalized reflected intensity (R), which is basically the output signal, is measured as a function of incident angle $\theta$ by keeping other parameters and components (such as frequency, metal layer, and dielectric layer) unchanged, then a

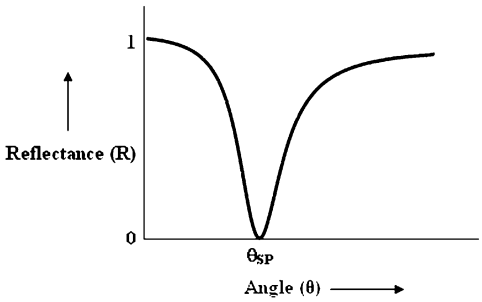


Fig. 7. Reflectance (R) as a function of angle of incidence $(\theta)$ at the prism-metal interface (angular interrogation). A sharp drop in reflected signal is observed at angle $\theta_{\rm res}$.

sharp dip is observed at resonance angle $\theta_{\rm SP}$ due to an efficient transfer of energy to surface plasmons (Fig. 7).

The minimum of the normalized reflected intensity (R) can be quantitatively described with the help of Fresnel's equations for the three-layer system p/m/s (see the appendix). Here "$p$" stands for high refractive index material prism, e.g., quartz prism, "$m$" stands for metal film of thickness $d_m$, and "$s$" stands for low index dielectric medium, e.g., air, water, etc.

The light wave is incident at an angle greater than the corresponding ATR angle. At this point, one has to remind that the energy conservation requires that $\mathrm{R}+\mathrm{A}+\mathrm{T}=1$, i.e., the sum of relative reflection, absorption, and transmission is unity. Since $\mathrm{T}=0$ at ATR, hence we are left with $\mathrm{A}+\mathrm{R}=1$ in the present case.

The light wave having passed the glass prism $(\varepsilon_p)$, is reflected partially at prism-metal interface. A part of the incident light wave energy traverses the metal film (of thickness $d_m$) as an exponentially decaying evanescent wave. At the metal-dielectric (m/s) interface, it induces the surface plasmon excitations, which radiate light back into the metal film. If the metal layer thickness $(d_m)$ is small, the backscattered field tends to increase. Since, this backscattered wave is out-of-phase with the incoming wave, the two interfere destructively and cause R to reduce. For minimum value of $d_m$, they compensate each other and R becomes equal to zero. Thus, the absorption A becomes equal to 1, i.e., whole radiation field is captured in the metal film. On the other hand, if the metal layer thickness is large enough, then the backscattered field disappears and R approaches to 1. It means that no absorption of incident light wave is taking place.

As a conclusive statement, one can say that the value of R depends on the combination of incident light frequency, angle of incidence, and the thickness of the metal layer.

### *G. Sensing Principle of SPR: Performance Parameters*

The sensing principle of SPR sensors is based on (4). For a given frequency of the light source and the dielectric constant of metal film one can determine the dielectric constant $(\varepsilon_s)$ of the sensing layer adjacent to metal layer by knowing the value of the resonance angle $(\theta_{\rm res})$. The resonance angle is determined by using angular interrogation method as discussed above. The resonance angle is very sensitive to variation in the refractive index (or, dielectric constant) of the sensing layer. Increase in refractive index of the dielectric sensing layer increases the resonance angle.

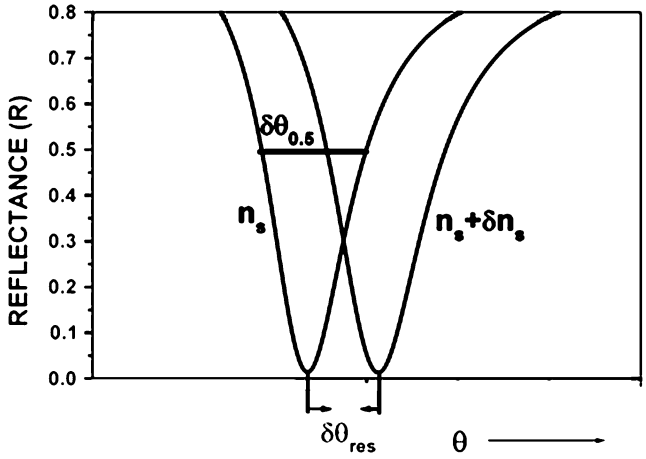


Fig. 8. The shift in resonance angle $(\delta\theta_{\rm res})$ with a change in refractive index of the sensing layer $(n_s)$ by $\delta n_s$. $\delta_{\theta_{0.5}}$ is the angular width of the curve at half reflectance for sensing layer refractive index $n_s$.

The performance of a SPR sensor is analyzed with the help of two parameters: sensitivity and detection accuracy or signal-to-noise ratio (SNR). For the best performance of the sensor, both parameters should be as high as possible to attain a perfect sensing procedure. Sensitivity of a SPR sensor depends on how much the resonance angle shifts with a change in refractive index of the sensing layer. If the shift is large, the sensitivity is large. Fig. 8 shows a plot of reflectance as a function of angle of the incident light beam for sensing layers with refractive indices $n_s$ and $n_s+\delta n_s$. Increase in refractive index by $\delta n_s$ shifts the resonance curve by $\delta\theta_{\rm res}$ angle. The sensitivity of a SPR sensor with angular interrogation is defined as

$$S_n = \frac{\delta\theta_{\rm res}}{\delta n_s}. \tag{5}$$

The detection accuracy or the SNR of a SPR sensor depends on how accurately and precisely the sensor can detect the resonance angle and, hence, the refractive index of the sensing layer. Prior to the evaluation of SNR, a commonly more natural and practical parameter $(S_L)$ related to the SNR in terms of the reflectivity (R) and resonance angle $(\theta_{\rm res})$ can be defined as

$$S_L = \frac{\delta R}{\delta\theta_{\rm res}}. \tag{6a}$$

This simply represents the slope of the reflectivity curve. The above parameter provides primary information regarding the detection sensitivity for SPR sensing system. The SNR is then derived soon, knowing the properties of the signals in the instrumentation chain. In other words, it is to be emphasized that the SNR is realized only at the end of the instruments chain, when one finally measures the resonance angle and the reflectivity with a real instrument. For instance, minimum angular resolution and minimum sensitivity of the optical detector used to measure the reflectivity are the important and critical parameters of a real instrument. Only if these above instrument parameters are known, one can make a statement about SNR.

Apart from the limitations of a real instrument, the accuracy of detection of resonance angle further depends on the width of the SPR curve. Narrower the SPR curve, higher is the detection accuracy. Therefore, if $\delta\theta_{0.5}$ is the angular width of the SPR

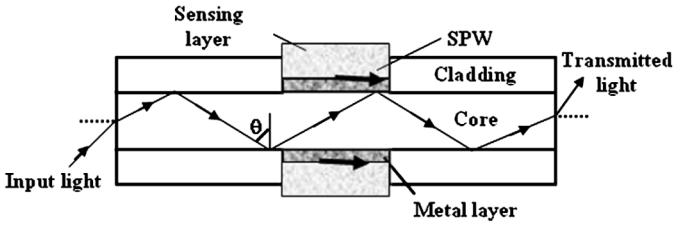


Fig. 9. Illustration of a typical fiber-optic SPR sensor.

response curve corresponding to 50% reflectance, the detection accuracy of the sensor can be assumed to be inversely proportional to $\delta\theta_{0.5}$ (Fig. 8). The SNR of the SPR sensor with angular interrogation is, thus, defined as [11]

$$\mathrm{SNR} = \frac{\delta\theta_{\mathrm{res}}}{\delta\theta_{0.5}}. \tag{6b}$$

Actual SNR of the real SPR sensing system critically depends on how well one measures the signals with real instruments.

## III. Fiber-Optic SPR Sensor

Introduction of optical fibers in the SPR sensing system is based on a very logical reason that guidance of light in optical fibers is also based on total internal reflection (TIR). Since, a prism is used in SPR sensing system in order to create TIR at the prism-metal interface; therefore, coupling prism used in the basic SPR theory can be conveniently replaced by the core of an optical fiber to design a fiber-optic SPR sensor. Among other important reasons are the advantages of optical fiber over coupling prism such as simple and flexible design, miniaturized sensor system, and capability of remote sensing. In general, the silicon cladding from a certain small portion (middle portion for most of the cases) of the fiber core is removed and is coated with a metal layer, which is further surrounded by a dielectric sensing layer (Fig. 9). The light from a polychromatic source, if spectral interrogation method is used, is launched into one of the ends of the optical fiber. The TIR takes place for the rays propagating with an angle in the range varying from the critical angle (depending upon the numerical aperture of the fiber and the light wavelength) to approximately 90°. Consequently, the evanescent field is generated, which excites the surface plasmons at the fiber core-metal layer interface. This coupling of the evanescent field with surface plasmons strongly depends upon light wavelength, fiber parameters, fiber geometry, and metal layer properties. For instance, coupling mechanism will be different for single-moded and multimoded optical fibers due to having different mode transmission properties depending upon the number of modes a fiber will support. Similarly, a straight fiber and a tapered fiber will show different strengths of light coupling because these fibers will show different penetration depths of the evanescent field due to having different geometrical configurations. A tapered fiber shows a substantial variation in evanescent field penetration along the tapered sensing region length whereas an untapered fiber exhibits uniform penetration of the evanescent field along the sensing region. Further, penetration of the evanescent field and, therefore, strength of light coupling with surface plasmons depends on an important fiber parameter known as numerical aperture, which is related to light acceptance limit of the fiber. Furthermore, unlike prism-based SPR geometry, the number of reflections for most of the angles is more than one for fiber-based SPR sensor geometry. Besides its angle, the number of reflections for any ray depends on other fiber parameters, namely, sensing region length, and fiber core diameter. The number of reflections directly affects the SPR curve width, therefore, performance parameters (SNR and sensitivity) of the sensor depends upon fiber properties in this way also. These different aspects related to fiber's optical and geometrical properties along with their advantages and disadvantages will be discussed in more detail at appropriate spaces in Section III of the review.

Finally, the spectrum of the light transmitted after passing through the SPR sensing region is detected at the other end. The sensing is accomplished by observing the wavelength corresponding to the dip in the spectrum. This wavelength is called as the resonance wavelength. A plot of resonance wavelength with the refractive index of the sensing layer gives the calibration curve of the fiber-optic SPR sensor. Unlike prism-based SPR sensor where angular interrogation method is used, the spectral interrogation method is generally used in the fiber-optic SPR senor because in the fiber-optic sensor all the guided modes are launched in the fiber.

## IV. Evolution of the Fiber-Optic SPR Sensors

The development of fiber-optic SPR sensors began in early nineties of last century. Among the first reports on fiber-optic SPR sensors was the one proposed by Villuendas and Palayo [12]. They presented the experimental results for sensitivity and dynamic range in the measurement of sucrose concentration in aqueous solution. Their work was followed by a four-layer fiber-optic SPR sensor with improved dynamic range and sensitivity compared with the three-layer sensor [13]. Soon after, a sensor based on excitation of SPR on the tip of a single-mode fiber was reported, which was based on the analysis of the state of polarization of the reflected beam [14]. At the same time, Jorgenson and Yee reported the theoretical as well as experimental work on a fiber-optic chemical sensor based on SPR by fabricating the probe on a highly multimoded optical fiber and using a white light source instead of a monochromatic one [15]. The sensor proposed by them was able to detect the changes in the parameters like bulk refractive index, film thickness, and film refractive index. Slightly later, an "in-line" optical fiber SPR sensor configuration was proposed for a large range of sensing applications [16]. As another significant application, the fiber-optic SPR sensor was used the first time to monitor the deposition of a multilayered cadmium arachidate Langmuir–Blodgett film [17]. Experiments showed that there were constant shifts in resonance wavelength as the number of monolayers was increased. This provided the method of calculating the film thickness by measuring the changes in SPR spectra.

The sensitivity and operating (or dynamic) range are the two important parameters of a practical sensor. Controlling of these two parameters is another important issue. It was addressed in the beginning years itself [18]. The sensitivity to refractive index was reported to be of the order of $10^{-5}$ RIU, while the dynamic range was found to be between 1.25 and 1.40 RIU. The dynamic range of the sensor can be tuned 1.00

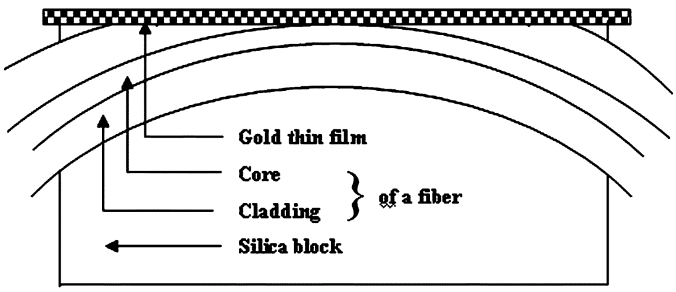


Fig. 10. Side polished single-mode optical fiber SPR sensor.

to 1.40 RIU by using a thin high refractive index overlay film. The above range includes gaseous samples as well. Moreover, the upper limit of the above range was extendible to 1.70 by the use of a sapphire core fiber. Soon after, a fiber-optic SPR remote sensor for the detection of tetrachloroethane was proposed by using a gas sensitive polymer film on the metal layer [19]. The sensor showed good response time (of 2 s), and reproducibility apart from a long-term stability (of more than three months). Around the same time, a fiber-optic SPR sensor with monochromatic excitation and angle of incidence was reported for the detection of refractive index [20]. The sensor was shown to have a resolution of the order of $10^{-4}$ RIU with dynamic range between 1.33 and 1.40. Later, the modeling of sensing signal was reported by the same group [21]. Homola and Slavik [22] reported a SPR sensor using side polished single-mode optical fiber and a thin metal overlayer (Fig. 10). The configuration of the probe is different from that shown in Fig. 9. The guided mode propagates in the optical fiber and excites a surface plasmon wave at the interface between the metal and a sensing medium, if the two modes are closely phase matched. As the surface plasmon wave is lossy, the coupling results in damping of the fiber mode. Because the coupling strength depends dramatically on the refractive index of the dielectric adjacent to the metal film (sensed medium), even small variations in the refractive index of the sensed medium may produce large changes in the attenuation of the fiber mode. Since surface plasmons are inherently TM-polarized waves, only fiber modes of the corresponding polarization state may be involved in this interaction (TM-polarized mode), while the modes with the orthogonal polarization state (TE-polarized mode) are attenuated only due to ohmic loss in the metal layer. The TE-polarized mode, the attenuation of which is not sensitive to changes in optical properties of the sensed medium, may be used as a reference. Such single-moded fiber-based SPR sensors are considered to be more sensitive, more accurate, and containing less noise in comparison to those with multimoded fibers. However, their fabrication is much more complex and sophisticated compared with those for multimoded fibers. The sensor was highly sensitive (sensitivity around $-2500$ dB/RIU for a refractive index range of 1.41–1.42 RIU) and a very small amount of sample was required for measuring the refractive index.

Study of self-assembled monolayers (SAMs) such as n-alkanethiol for the protection of silver film due to oxidation on fiber core was carried out [23]. Such thiol monolayers were found to be capable of protecting silver layer from oxidation. Further, the sensor with SAM was shown to have no ageing problem and had high stability. The SAM was later used in a fiber-optic SPR sensor for gas detection [24]. For detecting gases and vapors, the dielectric medium consisted of polyfluoroalkylsiloxane, was deposited over SAM. Halogenated hydrocarbons such as trichloroethylene, carbon tetrachloride, chloroform, and methylene chloride were tested with detection limits of 0.3%, 0.7%, 1%, and 2%, respectively. Response time of the sensor was less than 2 min. A side-polished single-mode fiber-optic SPR sensor discussed above was further modified [25]. In the modified design, the output end of the fiber was made reflecting. Therefore, in the modified sensor, instead of measuring transmitted light, the back reflected light from the mirrored end face of the fiber was detected. The operation range of the sensor was tuned toward aqueous media by using a thin tantalum pentaoxide overlayer. The resolution of the sensor was of the order of $10^{-4}$ RIU. Another sensor based on different configuration and reported around the same time showed the resolution of the order of $10^{-5}$ RIU using a single-mode fiber [26]. In this sensor, the fiber has one end polished at an angle relative to the longitudinal axis and coated with a thin gold film. The spatial SPR was observed by allowing the guided light to diffract out of the fiber probe. The resonance effect depends on the wavelength and the refractive index changes in the medium next to the metallic film at the fiber tip. Another single-mode fiber SPR sensor was reported for the measurement of refractive index [27]. The sensor can be used as a spectral, as well as an amplitude sensor. The theoretical analysis presented was based on the equivalent planar waveguide approach along with mode propagation and expansion method. In the mean time, chemical sensing with gold-coated SPR fiber-optic sensor was proposed [28]. Theoretical simulations showed that the proposed configuration allowed reaching a thirtyfold increase in sensitivity in comparison to the previous SPR-based sensors. Similarly, a simple quasi-geometric model to analyze the behavior of compound waveguide structures used as fiber-optic SPR sensors was reported [29]. The model took the nonmonochromatic nature of the light source.

The effect of polarization of the incident light in a multimode fiber is another critical factor in context of an SPR sensor. An important research work was carried out in this direction [30]. A three-dimensional skew ray model was developed to completely explain the experimental phenomenon for an intrinsic SPR multimode fiber sensor. The polarization of light source does not have much influence, while the SPR probe is far from the input end of the fiber. The model was important to explain the variations of the refractive index of the bulk medium and thickness of the thin dielectric layer. As another crucial development, gold island fiber-optic SPR sensor was proposed [31]. The fundamental optical absorbance at around 535 nm for gold particles was shown to shift if the fiber was immersed in different media.

The other configuration studied for SPR sensor was metal-coated tapered fiber for refractive index sensing [32]. Quasi-circular polarization insensitive devices and asymmetric polarization sensitive devices were fabricated and their characteristics as refractive index sensors were measured. High sensitivity of both

and their feasibility of using as wavelength—output or amplitude—output sensors were demonstrated. A novel probe based on monochromatic skew ray excitation of SPR was shown as a whole surface probe [33]. It was able to monitor the SAM formation and the immunoassay. A fiber-optic SPR sensor based on spectral interrogation in a side polished single-mode fiber using depolarized light was reported [34]. The sensor was able to measure refractive index variation as small as $10^{-7}$. Suitability of the sensor for biosensing was demonstrated by detecting IgG through respective monoclonal antibodies immobilized on the SPR sensor surface. Lin *et al.* [35] developed a fiber-optic sensor based on silver for chemical and biological applications. The range of refractive index was shifted down by coating an overlay of zirconium acetate on the silver surface by sol-gel method. The SPR sensor was reported to operate in the aqueous media with the detectable range of refractive indices of 1.33 to 1.36. A SAM of long chain thiol was introduced to cover the surface of silver in order to prevent it from deterioration.

A novel theoretical approach was applied to provide a better understanding of surface plasmon excitation in fiber-optic sensors [36]. The model was based on the calculation of the proposed fields in the waveguide structures and that enabled to evaluate the optical power loss from energy conservation considerations. The agreement of theoretical results with experimental data of real sensors was reported to be very good. Further, another improvement was made in context of fiber-optic SPR biosensor when the fast detection of Staphylococcal enterotoxin B (SEB) was reported [37]. The biosensor was based on side polished single-mode fiber and was able to detect ng/ml concentrations of SEB in less than 10 min. As another important development, an SPR sensor using an optical fiber with an inverted Graded-Index profile was proposed [38]. Both the simulation and experiments showed that the sensor exhibited high sensitivity for changes of the surrounding media in a RI range from 1.33 to 1.39. A fiber-optic SPR sensor for the detection of hydrogen was reported [39]. A thin palladium layer deposited on the metal coated core of a multimode fiber was used as the transducer. The modification of the SPR was due to variation in the complex permittivity of palladium in contact with gaseous hydrogen. This effect was enhanced by using selective injection of high-order modes in the fiber through a collimated beam on the input end of the fiber. Measurements of concentrations as low as 0.8% of hydrogen in pure nitrogen were reported. The response time varied between 3 s for pure hydrogen and 300 s for the lowest concentrations.

The use of single-mode polarization maintaining fiber (PMF) for SPR sensors was another milestone [40]. The above structure utilized both polarization-separation and broadband radiation depolarization in PMFs to enhance sensor's stability. The effect of polarization cross coupling was also analyzed. The experimental resolution of the sensors was of the order of $4 \times 10^{-6}$ RIU. A fiber-optic sensor with nanocomposite multilayered polymer and nanoparticle ultrathin films was reported for biosensing [41].

A new approach of hetero-core structure for a fiber-optic SPR sensor was introduced [42]. The hetero-core structured fiber-optic SPR probe consists of two fibers with different core diameter connected by thermal fusion splicing (Fig. 11). This

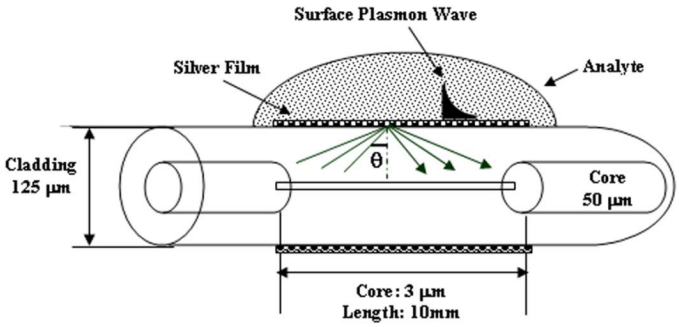


Fig. 11. Hetero-core structured optical fiber sensor, with the silver layer of 50 nm thickness on the cladding surface of the single-mode fiber.

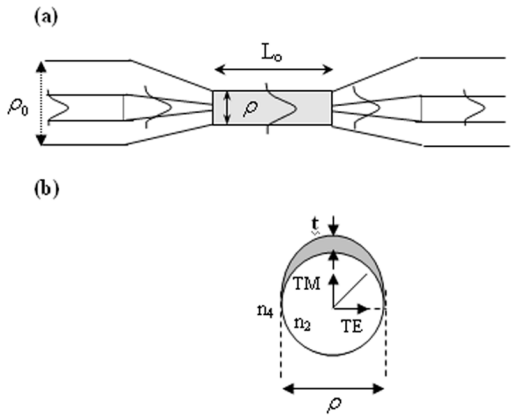


Fig. 12. (a) Single-mode tapered fiber with uniform waist. (b) Cross section of the waist after metallic coating.

was done, deliberately, to leak the transmitted power into the cladding layer of small core diameter fiber so that the leaked light may induce an optical evanescent wave required for SPR excitation. Silver was deposited around the cladding surface for SPR excitation. The spectral interrogation method was used to sense the refractive index. The most beneficial finding with this new sensing structure is its simplicity in the sensor fabrication. Additionally, because this structure has no need to eliminate the cladding layer of fiber, the fabricated fiber sensor probe is able to provide the characteristic advantage of optical fibers for remote monitoring. Next, a fiber-optic SPR sensor with asymmetric metal coating on a uniform waist single-mode tapered fiber, as shown in Fig. 12, was reported [43]. Due to the varying film thickness, the sensor transmission spectrum exhibited multiple resonance dips. The multiple dips increase the dynamic range of the sensor. A fiber-optic conical microsensor for SPR using chemically etched single-mode fiber was reported [44]. The probe was prepared by coating a gold-metallic film on the etched portion of the fiber containing conical core (Fig. 13). When the SAMs were applied on the metallic surface in order to avoid any adsorption or contamination, the sensor responded to the refractive index range of 1.33–1.40 with a sensitivity of 0.008 RIU. The issues related to the calibration of fiber-optic SPR sensors in aqueous systems were also addressed [45]. Among the biosensors, a real-time fiber-optic SPR sensor to detect biologically relevant concentrations of myglobin and cardiac troponin I in less than 10 min was proposed [46]. Further, work on robust SPR fiber-optic sensor [47], and fiber-optic

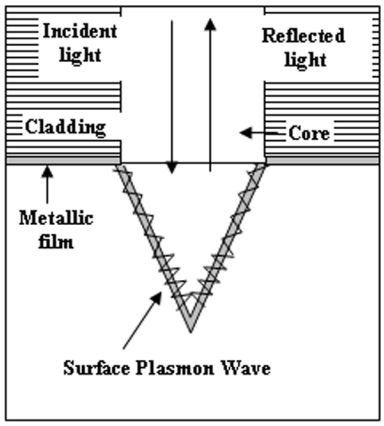


Fig. 13. Fiber-optic SPR microsensor.

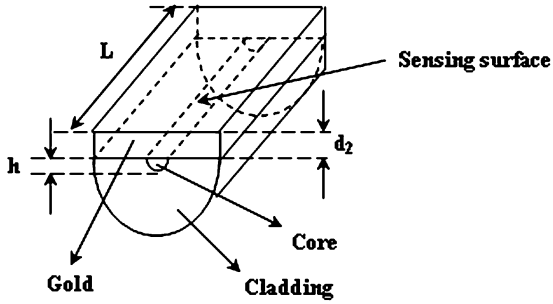


Fig. 14. ID-type optical fiber SPR sensor probe.

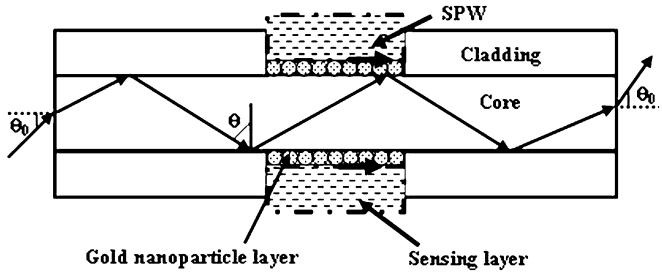


Fig. 15. A fiber-optic SPR sensor with metal nanoparticle layers.

microsensor based on white-light SPR excitation [48] were reported. A comprehensive model of on absorption-based fiber-optic SPR sensor for the detection of concentration of chemicals was proposed [49].

Fast responding fiber-optic SPR biosensor [50], analysis of a fiber-optic SPR sensor based on a crossing point of the two SPR spectra obtained from the sample fluid and the deionized water [51], the application of single-crystal sapphire-fiber-optic SPR sensor in the extreme environment [52] are some of the other advancements in this area. The use of tapered fiber-optic SPR sensor for vapor and liquid phase detection [53] is another important advancement. This technique of tapered-fiber employs a fiber-optic SPR probe with a modified geometry to tune the SPR coupling wavelength-angle pair. The observed composite spectrum includes two distinct SPR dips associated with surface plasmons excited in the gas and liquid active regions. This sensor is able to detect refractive index changes in both vapor and liquid phases individually by simultaneous monitoring SPR coupling wavelengths from the two sensing surfaces. The most important advantage of such dual-tapered and tetra-tapered fiber-optic SPR sensors lies in the simultaneous detection of liquid and vapor phases. However, as a big advantage, detection accuracy (i.e., SNR) is bound to decrease due to an increase in the number of reflections followed by the SPR curve broadening for tapered fiber geometry. Application of D-type optical fiber sensor based on heterodyne interferometry has also been a very interesting addition to the fiber-optic SPR sensor technology [54], [55]. The above design of sensor (Fig. 14) is valuable as it may reach the sensitivity of the order of $10^{-6}$ RIU. Further, a high resolution, $7 \times 10^{-7}$ RIU, refractive index sensing has been achieved by means of a multiple-peak SPR fiber-optic sensor [56]. A detailed sensitivity analysis along with performance optimization for multilayered fiber-optic SPR concentration sensor has been reported [57]. The sensitivity and SNR analysis of a fiber-optic SPR refractive index sensor has been carried out for different conditions related to metal layer, optical fiber, and light launching conditions along with an extension to remote sensing [58]. Development of a SPR-based fiber-optic sensor for bittering component (Naringin) has been recently reported [59].

Among the most recent developments is the application of nanoparticle films in fiber-optic SPR sensors. The analyses of the fiber-optic SPR sensor with metal-host nanoparticle layers (Fig. 15) [60] and silver-gold alloy layers [61] have been reported. The sensor with metal nanoparticle layer was found to have better performance than a similar sensor with bulk metal layer. Also, Ag-Au nanoparticle alloy-based sensor was found to be more sensitive and accurate in comparison to that with metal-host nanoparticle layers. Furthermore, the application of localized surface plasmon resonance (LSPR) in optical fiber sensors [62] and a colloidal gold-modified long-period fiber grating for chemical and biochemical sensing [63] have been a crucial advancement. Long-period fiber gratings (LPFG) offer a variety of applications in sensors owing to their low insertion losses, low back-reflection, polarization independence, and relatively simple fabrication. Among the main advantages of the LPFG-based SPR sensors is their simple construction and ease of use. Moreover, the sensor has the potential capability for on-site and remote sensing, can be easily multiplexed to enable high-throughout screening of bimolecular interactions, and has the potential use for disposable sensors. The above sensor with long-period fiber grating has shown a detection limit for anti DNP (dinitrophenyl compound) of $9.5 \times 10^{-9}$ M.

Among the other techniques, fiber Bragg gratings (FBGs) have also found applications in SPR sensing [64]. A novel technique of FBG assisted surface plasmon polariton (SPP) sensor has been proposed [65]. As another advance in this direction, the theoretical model of a new hollow core fiber sensor based on the specific properties of the SPP excited with a FBG is proposed [66]. The main principle of operation of this new device is based on the efficient energy transfer between the fiber waveguide mode (FWM) and the surface plasmon-polariton (SPP) provided by a properly designed short-period FBG imprinted

into a waveguide fiber layer of a specially designed hollow core optical fiber. The waveguide fiber layer is the dielectric layer of the fiber with the highest refractive index. The FWM is a fiber mode oscillating in this layer and exponentially decaying in all other fiber layers. The simulations are done with the help of coupled mode theory and performed for well-developed telecom wavelength ranges. These new models based on FBG may be able to design a highly flexible sensor system.

Recently, a new waveguide model of LSPR-based planar multireflection sensing system with gold nanospheres has been proposed [67]. In this sensing system, a strong enhancement of LSPR was observed with striking linearity and reproducibility by using a metallic layer of 20–30 nm gold nanoparticles. The feasibility of a fiber-optic SPR sensor for the determination of salinity has also been reported [68]. The effect of temperature on the performance of a fiber-optic SPR sensor has been theoretically studied in great detail [69] by incorporating the thermo-optic effects is metal layer, fiber core, and sensing layer. In a similar fashion, a model for fiber-optic SPR sensor for temperature detection has also been proposed [70]. Recently, a comparative study for the properties and surface characterization of a SPR-based fiber-optic sensor has been reported for different metals such as Au, Ag, Cu, and Al [71].

In recent times, SPR sensors based on photonic crystal waveguide [72] has been proposed. In the photonic crystal waveguide-based SPR sensor, plasmons on a surface of a thin metal film are excited by a Gaussian-like leaky mode of an effectively single-mode photonic crystal waveguide. It has been demonstrated that effective refractive index of a waveguide core mode can be designed to be considerably smaller than that of a core material, enabling efficient phase matching with plasmons at any wavelength of choice, while retaining highly sensitive response to changes in the refractive index of an analyte layer. This is quite an ideal technique for the development of portable SPR biochemical sensors. As another crucial advancement, the concept of a microstructured optical fiber-based SPR sensor with optimized microfluidics is proposed [73]. In this design, plasmons on the inner surface of large metallized channels containing analyte can be excited by a fundamental mode of a single-mode microstructured fiber. Phase matching between plasmon and a core mode is enforced by introducing air filled microstructure into the fiber core, thus allowing tuning of the modal refractive index and its matching with that of a plasmon. Sensitivity studies show that refractive index changes of $10^{-4}$ RIU leads to easily detectable 1% change in the transmitted light intensity.

## V. Future Scope of Work in Fiber-Optic SPR Sensors

Fiber-optic SPR sensors are bound to encounter more advancement in future, especially in biosensors, nanosensors, and photonic crystal-assisted sensors. All these fields have a vast opened area of research in context of fiber-optic SPR sensors.

The future of SPR-based fiber-optic biosensors will be driven by the need of the consumers, and hence it is important that the sensor should be made more consumers friendly. The areas in SPR-based fiber-optic biosensor, which really needs to be addressed presently, and which throws a challenge to the researchers working in this field is its specificity, i.e., how can a sensor be used to detect specific molecules from groups of molecules. Bimolecular recognition molecules may exhibit affinity to similar types of other unwanted molecules present in a given system. These unwanted molecules will react with the biosensors and will alter the refractive index, hence, affecting the different important parameter such as sensitivity, detection accuracy, reproducibility, etc., of the biosensor. If the concentration of unwanted molecules is high, then sensor response is more affected by it rather then by the molecule we want to detect. The other challenge lies in the nonspecific interactions between sensor surface with unwanted molecules and background refractive index variations. These variations can be because of temperature, humidity, and compositional fluctuations. The important issue, which eagerly waits the commercialization of SPR-based fiber-optic biosensor, is its use in the out of laboratory environment. To use the biosensors in field, mobile analytical systems need to be developed, which should enable rapid detection of given biological entity. Future development of these systems requires significant advances in miniaturization of biosensing platform, high specificity, robustness, and user friendliness.

On a similar note, nanoparticle-based fiber-optic SPR sensors are also due to get attention in the future. The technique of LSPR with metal nanoparticle layers has shown a lot of promise. Further optimization of the crucial factors and parameters to better the sensor's performance is required. New combinations such as metal-semiconductor nanocomposite, different bimetallic alloys (with nanoparticles of different metals such as Cu, Au, Ag, and Al, etc.) are to be used in SPR-based fiber-optic sensors. The added phenomena like Surface Enhanced Raman Scattering (SERS) are also there to have a look into. The scope of fiber-optic SPR sensors based on metal nanoparticle layers has to be extended for the detection of other parameters such as temperature, humidity, etc. The collaboration of fiber gratings and LSPR technique is another candidate for further work in this area.

Finally, photonic crystal fiber-based SPR sensors are bound to find new heights in the coming future due to their unique optical properties such as omnidirectionality, negative refractive indices, and gapless guidance.

## VI. Conclusion

The present paper is devoted to a comprehensive review of the SPR-based fiber-optic sensors. The collaboration of SPR technique and optical fiber technology has brought a lot of advancements in sensing of various physical, chemical, and biochemical parameters. We have tried to put forward a chronologically collective and systematic evolution of fiber-optic SPR sensors reported in the last 20 years or so. We believe that the present review will provide the researchers valuable information regarding fiber-optic SPR sensors and encourage them to take this area for further research and development.

## Appendix

The three-layer Fresnel equation for the reflected light intensity (R) is given by (Fig. 5)

$$\mathrm{R} = \left| \frac{r_{pm} + r_{ms} \exp(2ik_{mz}d_m)}{1 + r_{pm}r_{ms} \exp(2ik_{mz}d_m)} \right|^2 . \tag{A1}$$

For p-polarization

$$r_{pm} = \frac{k_{pz}\varepsilon_m - k_{mz}\varepsilon_p}{k_{pz}\varepsilon_m + k_{mz}\varepsilon_p} \tag{A2}$$

and

$$r_{ms} = \frac{k_{mz}\varepsilon_s - k_{sz}\varepsilon_m}{k_{mz}\varepsilon_s + k_{sz}\varepsilon_m}. \tag{A3}$$

Further

$$k_{jz} = \left(\varepsilon_j \frac{\omega^2}{c^2} - k_x^2\right)^{1/2} \tag{A4}$$

with

$$k_x = \sqrt{\varepsilon_p}\frac{\omega}{c}\sin\theta. \tag{A5}$$

In the above expressions (A1)–(A5), $r_{pm}$ and $r_{ms}$, respectively, are the amplitude reflection coefficients for the prism-metal layer and metal layer-sensing layer interfaces; $\varepsilon_j$ is the dielectric constant of $j$th medium; $k_{jz}$ is the wave propagation vector in $z$-direction, i.e., perpendicular to the interface in the medium $j$; $k_x$ is the evanescent wave propagation constant parallel to the metal layer-sensing layer interface; $d_m$ is the thickness of the metal layer; $\omega$ is the angular frequency of the incident light, and $c$ is the speed of light.

In general, prism is considered to be nondispersive. However, for the sake of completeness, the wavelength dependence of the refractive index $(n_p = \sqrt{\varepsilon_p})$ of the fused silica prism is given by Sellmeier dispersion relation

$$n_1(\lambda) = \sqrt{1 + \frac{a_1\lambda^2}{\lambda^2 - b_1^2} + \frac{a_2\lambda^2}{\lambda^2 - b_2^2} + \frac{a_3\lambda^2}{\lambda^2 - b_3^2}} \tag{A6}$$

where $a_1, a_2, a_3, b_1, b_2,$ and $b_3$ are Sellmeier coefficients. The value of coefficients are $\mathrm{a1} = 0.004679148, \mathrm{a2} = 0.01351206, \mathrm{a3} = 97.93400, \mathrm{b1} = 0.6961663, \mathrm{b2} = 0.4079426, \mathrm{b3} = 0.8974794$. [74].

For the dispersion in metal layer, one may use the Drude model, given as [75]

$$\varepsilon_m(\lambda) = \varepsilon_{mr} + i\varepsilon_{mi} = 1 - \frac{\lambda^2\lambda_c}{\lambda_p^2(\lambda_c + i\lambda)} \tag{A7}$$

where $\lambda_p$ and $\lambda_c$ denote the plasma wavelength and collision wavelength, respectively. For instance, the following values of the plasma wavelength and collision wavelength for gold are used $\lambda_p = 1.6826 \times 10^{-7}$ m and $\lambda_c = 8.9342 \times 10^{-6}$ m.

According to the Kretschmann theory, for p-polarized light, the reflected light intensity given by (A1) may be transformed to [76]

$$\mathrm{R} = 1 - \frac{4k_{0p}{''}k_{Rp}{''}}{(k_x - k_{mp}{'})^2 + k_{mp}{''}^2} \tag{A8}$$

with

$$k_{mp} = k_{mp}{'} + ik_{mp}{''} = k_{0p} + k_{Rp} \tag{A9}$$

$$k_{0p} = k_{0p}{'} + ik_{0p}{''} = \frac{\omega}{c}\sqrt{\frac{\varepsilon_m\varepsilon_s}{\varepsilon_m + \varepsilon_s}} \tag{A10}$$

and

$$k_{Rp} = k_{Rp}{'} + ik_{\mathrm{R}p}{''} = -\frac{\omega}{c}(r_{pm})_{k_x} = k_0 \times \left(\frac{2}{\varepsilon_m - \varepsilon_s}\right)\left(\frac{\varepsilon_m\varepsilon_s}{\varepsilon_m + \varepsilon_s}\right)^{3/2} \times \exp\left[-i\frac{4\pi d_m}{\lambda}\frac{\varepsilon_m}{(\varepsilon_m + \varepsilon_s)^{1/2}}\right] \tag{A11}$$

where $k_{mp}$ is the complex wave vector of the surface plasmon wave generated under the Kretschmann ATR configuration; $k_{0p}$ is the complex wave vector of the surface plasmon wave in vacuum i.e., in the absence of the prism; $k_{Rp}$ is the perturbation to $k_{0p}$ in the presence of prism. The imaginary part of $k_{0p}$ is known as the intrinsic damping $(\gamma_i)$ and it represents the Joule loss in the metal layer. Similarly, the imaginary part of $k_{Rp}$ is radiative damping $(\gamma_{\mathrm{rad}})$ and represents the leakage loss of the SPW back into the prism.

Taking all the above expressions into consideration, (A1) for R can be approximated in the region of the resonance by another Lorentzian type of expression, which is essential in revealing its physical meaning, given by

$$R = 1 - \frac{4\gamma_i\gamma_{\mathrm{rad}}}{(k_x - k_{mp}{'})^2 + (\gamma_i + \gamma_{\mathrm{rad}})^2}. \tag{A12}$$

Equation (A12) demonstrates that R passes through a minimum that becomes zero for

$$\gamma_i = \gamma_{\mathrm{rad}}. \tag{A13}$$

The radiative damping, $\gamma_{\mathrm{rad}}$, which is the imaginary part of $k_{Rp}$, depends on the thickness of the metal layer [according to (A11)] such that it is large for small thickness and *vice versa*. Thus, above expression suggests that the exact matching condition also depends on the thickness of the metal layer. There is always a certain thickness $(d_{\min})$ of metal layer at a certain frequency for which R becomes zero. Further, this matching condition depends on frequency in two ways: first, a direct dependence as frequency $\omega$ is present in the expression for $k_{Rp}$, and second, an extrinsic dependence is also apparent due to frequency dependent metal dielectric function $(\varepsilon_m)$. At a certain wavelength (or frequency), internal damping $(\gamma_i)$ remains constant for any metal layer thickness, whereas internal damping varies with thickness. Therefore, resonance point is different for different values of metal layer thickness.

## REFERENCES


[1] J. Zenneck, "Uber die Fortpflanztmg ebener elektro-magnetischer Wellen langs einer ebenen Leiterflache und ihre Beziehung zur drahtlosen Telegraphie," *Annals der Physik*, vol. 23, pp. 846–866, 1907.

[2] A. Sommerfeld, "Propagation of Waves in Wireless Telegraphy," *Annals der Physik*, vol. 28, pp. 665–736, 1909.

[3] R. H. Ritchie, "Plasma losses by fast electrons in thin films," *Phys. Rev.*, vol. 106, pp. 874–881, 1957.

[4] C. J. Powell and J. B. Swan, "Effect of oxidation on the characteristic loss spectra of aluminum and magnesium," *Phys. Rev.*, vol. 118, pp. 640–643, 1960.

[5] E. A. Stern and R. A. Ferrell, "Surface plasma oscillations of a degenerate electron gas," *Phys. Rev.*, vol. 120, pp. 130–136, 1960.

[6] A. Otto, "Excitation of nonradiative surface plasma waves in silver by the method of frustrated total reflection," *Zeitschrift für Physik*, vol. 216, pp. 398–410, 1968.

[7] E. Kretschmann and H. Reather, "Radiative decay of non-radiative surface plasmons excited by light," *Zeitschrift für Naturforschung*, vol. 23, pp. 2135–2136, 1968.

[8] J. Homola, S. S. Yee, and G. Gauglitz, "Surface plasmon resonance sensors: Review," *Sens. Actuators B*, vol. 54, pp. 3–15, 1999.

[9] R. Ince and R. Narayanaswamy, "Analysis of the performance of interferometry, surface plasmon resonance, and luminescence as biosensors and chemosensors," *Anal. Chim. Acta*, vol. 569, pp. 1–20, 2006.

[10] O. S. Wolfbeis, "Fiber-optic chemical sensors and biosensors.," *Anal. Chem.*, vol. 78, pp. 3859–3873, 2006.

[11] S. A. Zynio, A. V. Samoylov, E. R. Surovtseva, V. M. Mirsky, and Y. M. Shirsov, "Bimetallic layers increase sensitivity of affinity sensors based on surface plasmon resonance," *Sensors*, vol. 2, pp. 62–70, 2002.

[12] F. Villuendas and J. Pelayo, "Optical fibre device for chemical seming based on surface plasmon excitridon," *Sens. Actuators A*, vol. 23, pp. 1142–1145, 1990.

[13] G. C. Aldea and J. Mateo, "Four-layer chemical fibre optic plasmon-based sensor," *Sens. Actuators B*, vol. 7, pp. 771–774, 1992.

[14] L. D. Maria, M. Martinelli, and G. Vegetti, "Fiber-optic sensor based on surface plasmon interrogation," *Sens. Actuators B*, vol. 12, pp. 221–223, 1993.

[15] R. C. Jorgenson and S. S. Yee, "A fiber-optic chemical sensor based on surface plasmon resonance," *Sens. Actuators B*, vol. 12, pp. 213–220, 1993.

[16] R. Alonso, F. Villuendas, J. Tornos, and J. Pelayo, "New 'in-line" optical-fibre sensor based on surface plasmon excitation," *Sens. Actuators A*, vol. 37, pp. 187–192, 1993.

[17] M. Mar, R. C. Jorgenson, S. Letellier, and S. S. Yee, "In-situ characterization of multilayered Langmuir-Blodgett films using a surface plasmon resonance fiber optic sensor," in *Proc. 15th Annu. Int. Conf. IEEE*, 1993, pp. 1551–1552.

[18] R. C. Jorgenson and S. S. Yee, "Control of the dynamic range and sensitivity of a surface plasmon resonance based fiber optic sensor," *Sens. Actuators A*, vol. 43, pp. 44–48, 1994.

[19] M. Niggemann, A. Katerkamp, M. Pellmann, P. Bolsmann, J. Reinbold, and K. Cammann, "Remote sensing of tetrachloroethene with a micro-fibre optical gas sensor based on surface plasmon resonance spectroscopy," in *Proc. 8th Int. Conf. Solid-State Sens. Actuators, Eurosensors IX*, Stockholm, Sweden, 1995, vol. 2, pp. 797–800.

[20] C. Ronot-Trioli, A. Trouillet, C. Veillas, and H. Gagnaire, "A monochromatic excitation of a surface plasmon resonance in an optical fibre refractive index sensor," in *Proc. 8th Int. Conf. Solid-State Sens. Actuators, Eurosensors IX*, Stockholm, Sweden, 1995, vol. 2, pp. 793–796.

[21] A. Trouillet, C. Ronot-Trioli, C. Veillas, and H. Gagnaire, "Chemical sensing by surface plasmon resonance in a multimode optical fibre," *Pure and Appl. Opt.*, vol. 5, pp. 227–237, 1996.

[22] J. Homola and R. Slavik, "Fibre-optic sensor based on surface plasmon resonance," *Electron. Lett.*, vol. 32, pp. 480–482, 1996.

[23] A. Abdelghani, J. M. Chovelon, J. M. Krafft, N. Jaffrezic-Renault, A. Trouillet, C. Veillas, C. Ronot-Trioli, and H. Gagnaire, "Study of self-assembled monolayers of n-alkanethiol on a surface plasmon resonance fibre optic sensor," *Thin Solid Films*, vol. 284–285, pp. 157–161, 1996.

[24] A. Abdelghani, J. M. Chovelon, N. Jaffrezic-Renault, C. Ronot-Trioli, C. Veillas, and H. Gagnaire, "Surface plasmon resonance fibre-optic sensor for gas detection," *Sens. Actuators B*, vol. 39, pp. 407–410, 1997.

[25] R. Slavík, J. Homola, and J. Ctyroký, "Miniaturization of fiber optic surface plasmon resonance sensor," *Sens. Actuators B*, vol. 51, pp. 311–315, 1998.

[26] E. Fontana, H. D. Dulman, D. E. Doggett, and R. H. Pantell, "Surface plasmon resonance on a single mode optical fiber," *IEEE Trans. Instrum. Measure.*, vol. 47, pp. 168–173, 1998.

[27] R. Slavík, J. Homola, and J. Ctyroký, "Single-mode optical fiber surface plasmon resonance sensor," *Sens. Actuators B*, vol. 54, pp. 74–79, 1999.

[28] E. Fontana, "Chemical sensing with gold coated optical fibers," in *Proc. Microw. Optoelectron. Conf.*, 1999, vol. 2, pp. 415–419.

[29] Ó. Esteban, M. C. Navarrete, A. González-Cano, and E. Bernabeu, "Simple model of compound waveguide structures used as fiber-optic sensors," *Opt. Lasers Eng.*, vol. 33, pp. 219–230, 2000.

[30] W. B. Lin, N. Jaffrezic-Renault, A. Gagnaire, and H. Gagnaire, "The effects of polarization of the incident light-modeling and analysis of a SPR multimode optical fiber sensor," *Sens. Actuators A*, vol. 84, pp. 198–204, 2000.

[31] F. Meriaudeau, A. Wig, A. Passian, T. Downey, M. Buncick, and T. L. Ferrell, "Gold island fiber optic sensor for refractive index sensing," *Sens. Actuators B*, vol. 69, pp. 51–57, 2000.

[32] A. Díez, M. V. Andrés, and J. L. Cruz, "In-line fiber-optic sensors based on the excitation of surface plasma modes in metal-coated tapered fibers," *Sens. Actuators B*, vol. 73, pp. 95–99, 2001.

[33] W. B. Lin, N. Jaffrezic-Renault, J. M. Chovelon, and M. Lacroix, "Optical fiber as a whole surface probe for chemical and biological applications," *Sens. Actuators B*, vol. 74, pp. 207–211, 2001.

[34] R. Slavík, J. Homola, J. Ctyroký, and E. Brynda, "Novel spectral fiber optic sensor based on surface plasmon resonance," *Sens. Actuators B*, vol. 74, pp. 106–111, 2001.

[35] W. B. Lin, M. Lacroix, J. M. Chovelon, N. Jaffrezic-Renault, and H. Gagnaire, "Development of a fiber-optic sensor based on surface plasmon resonance on silver film for monitoring aqueous media," *Sens. Actuators B*, vol. 75, pp. 203–209, 2001.

[36] O. Esteban, R. Alonso, C. Navarrete, and C. A. Gonzalez-Cano, "Surface plasmon excitation in fiber-optics sensors: A novel theoretical approach," *J. Lightw. Technol.*, vol. 20, pp. 448–453, 2002.

[37] R. Slavík, J. Homola, and E. Brynda, "A miniature fiber optic surface plasmon resonance sensor for fast detection of staphylococcal enterotoxin B," *Biosens. Bioelectron.*, vol. 17, pp. 591–595, 2002.

[38] F. Bardin, I. Kasik, A. Trouillet, V. Matejec, H. Gagnaire, and M. Chomat, "Surface plasmon resonance sensor using an optical fiber with an inverted graded-index profile," *Appl. Opt.*, vol. 41, pp. 2514–2520, 2002.

[39] X. Bévenot, A. Trouillet, C. Veillas, H. Gagnaire, and M. Clément, "Surface plasmon resonance hydrogen sensor using an optical fibre," *Measure. Sci. Technol.*, vol. 13, pp. 118–124, 2002.

[40] M. Piliarik, J. Homola, Z. Maníková, and J. Ctyroký, "Surface plasmon resonance sensor based on a single-mode polarization-maintaining optical fiber," *Sens. Actuators B*, vol. 90, pp. 236–242, 2003.

[41] P. S. Grant, S. Kaul, S. Chinnayelka, and M. J. McShane, "Fiber optic biosensors comprising nanocomposite multilayered polymer and nanoparticle ultrathin films," in *Proc. IEEE 25th Annu. Int. Conf.*, 2003, vol. 4, pp. 2987–2990.

[42] M. Iga, A. Seki, and K. Watanabe, "Hetero-core structured fiber optic surface plasmon resonance sensor with silver film," *Sens. Actuators B*, vol. 101, pp. 368–372, 2004.

[43] D. Monzón-Hernández, J. Villatoro, D. Talavera, and D. Luna-Moreno, "Optical-fiber surface-plasmon resonance sensor with multiple resonance peaks," *Appl. Opt.*, vol. 43, pp. 1216–1220, 2004.

[44] K. Kurihara, H. Ohkawa, Y. Iwasaki, O. Niwa, T. Tobita, and K. Suzuki, "Fiber-optic conical microsensors for surface plasmon resonance using chemically etched single-mode fiber," *Analytica Chimica Acta*, vol. 523, pp. 165–170, 2004.

[45] D. J. Gentleman, L. A. Obando, J. F. Masson, J. R. Holloway, and K. Booksh, "Calibration of fiber optic based surface plasmon resonance sensors in aqueous systems," *Analytica Chimica Acta*, vol. 515, pp. 291–302, 2004.

[46] J. F. Masson, L. A. Obando, S. Beaudoin, and K. S. Booksh, "Sensitive and real-time fiber-optic-based surface plasmon resonance sensors for myoglobin and cardiac troponin I," *Talanta*, vol. 62, pp. 865–870, 2004.

[47] L. A. Obando, D. J. Gentleman, J. R. Holloway, and K. S. Booksh, "Manufacture of robust surface plasmon resonance fiber optic based dip-probes," *Sens. Actuators B*, vol. 100, pp. 439–449, 2004.

[48] B. Grunwald and G. Holst, "Fibre optic refractive index microsensor based on white-light SPR excitation," *Sens. Actuators A*, vol. 113, pp. 174–180, 2004.

[49] A. K. Sharma and B. D. Gupta, "Absorption-based fiber optic surface plasmon resonance sensor: A theoretical evaluation," *Sens. Actuators B*, vol. 100, pp. 423–431, 2004.

[50] R. Micheletto, K. Hamamoto, S. Kawai, and Y. Kawakami, "Modeling and test of fiber-optics fast SPR sensor for biological investigation," *Sens. Actuators A*, vol. 119, pp. 283–290, 2005.

[51] W. Tsai, Y. Tsao, H. Lin, and B. Sheu, "Cross-point analysis for a multimode fiber sensor based on surface plasmon resonance," *Opt. Lett.*, vol. 30, pp. 2209–2211, 2005.

[52] Y. C. Kim, J. F. Masson, and K. S. Booksh, "Single-crystal sapphire-fiber optic sensors based on surface plasmon resonance spectroscopy for in situ monitoring," *Talanta*, vol. 67, pp. 908–917, 2005.

[53] Y. Kim, W. Peng, S. Banerji, and K. S. Booksh, "Tapered fiber optic surface plasmon resonance sensor for analyses of vapor and liquid phases," *Opt. Lett.*, vol. 30, pp. 2218–2220, 2005.

[54] S. F. Wang, M. H. Chiu, and R. S. Chang, "Numerical simulation of a D-type optical fiber sensor based on the Kretschmann's configuration and heterodyne interferometry," *Sens. Actuators B*, vol. 114, pp. 120–126, 2006.
[55] S. F. Wang, M. H. Chiu, J. C. Hsu, R. S. Chang, and F. T. Wang, "Theoretical analysis and experimental evaluation of D-type optical fiber sensor with a thin gold film," *Opt. Commun.*, vol. 253, pp. 283–289, 2005.
[56] D. M. Hernández and J. Villatoro, "High-resolution refractive index sensing by means of a multiple-peak surface plasmon resonance optical fiber sensor," *Sens. Actuators B*, vol. 115, pp. 227–231, 2006.
[57] B. D. Gupta and A. K. Sharma, "Sensitivity evaluation of a multi-layered surface plasmon resonance-based fiber optic sensor: A theoretical study," *Sens. Actuators B*, vol. 107, pp. 40–46, 2005.
[58] A. K. Sharma and B. D. Gupta, "On the sensitivity and signal-to-noise ratio of a step-index fiber optic surface plasmon resonance sensor with bimetallic layers," *Opt. Commun.*, vol. 45, pp. 159–169, 2005.
[59] Rajan, S. Chand, and B. D. Gupta, "Fabrication and characterization of a surface plasmon resonance based fiber-optic sensor for bittering component—Naringin," *Sens. Actuators*, vol. 115, pp. 344–348, 2006.
[60] A. K. Sharma and B. D. Gupta, "Fiber optic sensor based on surface plasmon resonance with nanoparticle films," *Photonics and Nanostructures: Fundamentals and Appl.*, vol. 3, pp. 30–37, 2005.
[61] A. K. Sharma and B. D. Gupta, "Fiber-optic sensor based on surface plasmon resonance with Ag-Au alloy nanoparticle films," *Nanotechnology*, vol. 17, pp. 124–131, 2006.
[62] L. K. Chau, Y. F. Lin, S. F. Cheng, and T. J. Lin, "Fiber-optic chemical and biochemical probes based on localized surface plasmon resonance," *Sens. Actuators B*, vol. 113, pp. 100–105, 2006.
[63] J. L. Tang, S. F. Cheng, W. T. Hsu, T. Y. Chiang, and L. K. Chau, "Fiber-optic biochemical sensing with a colloidal gold-modified long period fiber grating," *Sens. Actuators B*, vol. 119, pp. 105–109, 2006.
[64] S. Jette-Charbonneau and P. Berini, "Theoretical performance of Bragg gratings based on long-range surface plasmon-polariton waveguides," *J. Opt. Soc. Amer. A*, vol. 23, pp. 1757–1767, 2006.
[65] G. Nemova and R. Kashyap, "Fiber Bragg grating assisted surface plasmon-polariton sensor," *Opt. Lett.*, vol. 24, pp. 3789–3796, 2006.
[66] G. Nemova and R. Kashyap, "Modeling of plasmon-polariton refractive-index hollow core fiber sensors assisted by a fiber Bragg grating," *J. Lightw. Technol.*, vol. 24, pp. 3789–3796, 2006.
[67] K. Hamamoto, R. Micheletto, M. Oyama, A. Ali-Umar, S. Kawai, and Y. Kawakami, "An original planar multireflection system for sensing using the local surface plasmon resonance of gold nanosphere," *J. Optics A: Pure and Applied Optics*, vol. 8, pp. 268–271, 2006.
[68] D. J. Gentleman and K. S. Booksh, "Determining salinity using a multimode fiber optic surface plasmon resonance dip-probe," *Talanta*, vol. 68, pp. 504–515, 2006.
[69] A. K. Sharma and B. D. Gupta, "Influence of temperature on the sensitivity and signal-to-noise ratio of a fiber optic surface plasmon resonance sensor," *Appl. Opt.*, vol. 45, pp. 151–161, 2006.
[70] A. K. Sharma and B. D. Gupta, "Theoretical model of a fiber optic remote sensor based on surface plasmon resonance for temperature detection," *Opt. Fiber Technol.*, vol. 12, pp. 87–100, 2006.
[71] M. Mitsushio, K. Miyashita, and M. Higo, "Sensor properties and surface characterization of the metal-deposited SPR optical fiber sensors with Au, Ag, Cu, and Al," *Sens. Actuators A*, vol. 125, pp. 296–303, 2006.
[72] M. Skorobogatiy and A. Kabashin, "Photon crystal waveguide-based surface plasmon resonance biosensor," *Appl. Phys. Lett.*, vol. 89, 2006, Article No. 143518.
[73] A. Hassani and M. Skorobogatiy, "Design of the microstructured optical fiber-based surface plasmon resonance sensors with enhanced microfluidics," *Opt. Express*, vol. 14, pp. 11616–11621, 2006.
[74] A. K. Ghatak and K. Thyagarajan, *An Introduction to Fiber Optics*. Cambridge, U.K.: Cambridge Univ. Press, 1999, pp. 85–87.
[75] J. Homola, "On the sensitivity of surface-plasmon resonance sensors with spectral interrogation," *Sens. Actuators B*, vol. 41, pp. 207–211, 1997.
[76] K. Kurihara and K. Suzuki, "Theoretical understanding of an absorption-based surface plasmon resonance sensor based on Kretschmann's theory," *Anal. Chem.*, vol. 74, pp. 696–701, 2002.

**Anuj K. Sharma** received the M.Sc. degree in physics from the Indian Institute of Technology, Roorkee, India, in 2001 and the Ph.D. degree in physics from the Indian Institute of Technology, New Delhi, India, in 2006.

Currently, he is a Research Associate at the Indian Institute of Technology, New Delhi. He has been a Research Fellow at the University Grants Commission, India, from 2002 to 2006. He has published more than ten research articles in international journals of repute. His areas of research are fiber-optic sensors, surface plasmon resonance (SPR), and metal nanoparticles.

Dr. Sharma has been a member of the Optical Society of America (OSA).

**Rajan Jha** received the M.Sc. degree in physics from the Indian Institute of Technology, New Delhi, India, in 2001. He is currently working towards the Ph.D. degree at the Indian Institute of Technology.

**B. D. Gupta** received his M.Sc. degree in physics from the Aligarh Muslim University, Aligarh, India, in 1975 and the Ph.D. degree in physics from the Indian Institute of Technology, New Delhi, India, in 1979.

In 1978, he joined the Indian Institute of Technology, where he is currently an Associate Professor of Physics. He has also worked at the University of Guelph (Canada) from 1982–1983, the University of Toronto (Canada) in 1985, and Florida State University in 1988. In 1993, he visited the Department of Electronic and Electrical Engineerin, University of Strathclyde (UK), to work on fiber-optic chemical sensors under the Indo-British Fiber Optics Project. In 1992, he was awarded the ICTP Associateship by the International Centre for Theoretical Physics, Trieste, Italy, which he held for eight consecutive years. In this capacity, he visited ICTP (Italy) in both 1994 and 1996. He is the authored of *Fiber Optic Sensors: Principles and Applications* (NIPA New Delhi, 2006) and is the Co-Editor of the *Asian Journal of Physics*, *Proceedings of SPIE* (USA) Vol. 3666 (1998), and *Advances in Contemporary Physics and Energy* (Supplement Volume) (Allied Publishers, New Delhi). He has published more than 60 research papers including four review articles in international journals of repute. His current area of interest is fiber-optic sensors.

Dr. Gupta is a member of the Optical Society of America and Life Member of the Optical Society of India and the Indian Chapter of ICTP. He is a recipient of the 1991 Gowri Memorial Award of the Institution of Electronics and Telecommunication Engineers (India).